NASA/TM—2006-214045 AIAA–2005–5687

Single Phase Passive Rectification Versus Active Rectification Applied to High Power Stirling Engines

Walter Santiago and Arthur G. Birchenough
Glenn Research Center, Cleveland, Ohio

March 2006

The NASA STI Program Office . . . in Profile

Since its founding, NASA has been dedicated to the advancement of aeronautics and space science. The NASA Scientific and Technical Information (STI) Program Office plays a key part in helping NASA maintain this important role.

The NASA STI Program Office is operated by Langley Research Center, the Lead Center for NASA's scientific and technical information. The NASA STI Program Office provides access to the NASA STI Database, the largest collection of aeronautical and space science STI in the world. The Program Office is also NASA's institutional mechanism for disseminating the results of its research and development activities. These results are published by NASA in the NASA STI Report Series, which includes the following report types:

- TECHNICAL PUBLICATION. Reports of completed research or a major significant phase of research that present the results of NASA programs and include extensive data or theoretical analysis. Includes compilations of significant scientific and technical data and information deemed to be of continuing reference value. NASA's counterpart of peer-reviewed formal professional papers but has less stringent limitations on manuscript length and extent of graphic presentations.

- TECHNICAL MEMORANDUM. Scientific and technical findings that are preliminary or of specialized interest, e.g., quick release reports, working papers, and bibliographies that contain minimal annotation. Does not contain extensive analysis.

- CONTRACTOR REPORT. Scientific and technical findings by NASA-sponsored contractors and grantees.

- CONFERENCE PUBLICATION. Collected papers from scientific and technical conferences, symposia, seminars, or other meetings sponsored or cosponsored by NASA.

- SPECIAL PUBLICATION. Scientific, technical, or historical information from NASA programs, projects, and missions, often concerned with subjects having substantial public interest.

- TECHNICAL TRANSLATION. English-language translations of foreign scientific and technical material pertinent to NASA's mission.

Specialized services that complement the STI Program Office's diverse offerings include creating custom thesauri, building customized databases, organizing and publishing research results . . . even providing videos.

For more information about the NASA STI Program Office, see the following:

- Access the NASA STI Program Home Page at ***http://www.sti.nasa.gov***

- E-mail your question via the Internet to help@sti.nasa.gov

- Fax your question to the NASA Access Help Desk at 301–621–0134

- Telephone the NASA Access Help Desk at 301–621–0390

- Write to:
  NASA Access Help Desk
  NASA Center for AeroSpace Information
  7121 Standard Drive
  Hanover, MD 21076

NASA/TM—2006-214045 AIAA–2005–5687

Single Phase Passive Rectification Versus Active Rectification Applied to High Power Stirling Engines

Walter Santiago and Arthur G. Birchenough
Glenn Research Center, Cleveland, Ohio

Prepared for the
Third International Energy Conversion Engineering Conference
sponsored by the American Institute of Aeronautics and Astronautics
San Francisco, California, August 15–18, 2005

National Aeronautics and
Space Administration

Glenn Research Center

March 2006

Acknowledgments

The authors wish to thank Scott Gerber, ZIN, Technologies, Inc., for his technical contributions in the simulation and power electronics areas applied to Stirling engines. Also, special thanks to Andy Brush, Brush Technology, for his contribution on the PMAD area.

Available from

NASA Center for Aerospace Information
7121 Standard Drive
Hanover, MD 21076

National Technical Information Service
5285 Port Royal Road
Springfield, VA 22100

Available electronically at http://gltrs.grc.nasa.gov

Single Phase Passive Rectification Versus Active Rectification Applied to High Power Stirling Engines

Walter Santiago and Arthur G. Birchenough
National Aeronautics and Space Administration
Glenn Research Center
Cleveland, Ohio 44135

Abstract

Stirling engine converters are being considered as potential candidates for high power energy conversion systems required by future NASA explorations missions. These types of engines typically contains two major moving parts, the displacer and the piston, in which a linear alternator is attached to the piston to produce a single phase sinusoidal waveform at a specific electric frequency. Since all Stirling engines perform at low electrical frequencies (less or equal to 100 Hz), space explorations missions that will employ these engines will be required to use dc power management and distribution (PMAD) system instead of an ac PMAD system to save on space and weight. Therefore, to supply such dc power an ac to dc converter is connected to the Stirling engine. There are two types of ac to dc converters that can be employed, a passive full bridge diode rectifier and an active switching full bridge rectifier.

Due to the inherent line inductance of the Stirling Engine-Linear Alternator (SE-LA), their sinusoidal voltage and current will be phase shifted producing a power factor below 1. In order to keep power the factor close to unity, both ac to dc converters topologies will implement power factor correction. This paper discusses these power factor correction methods as well as their impact on overall mass for exploration applications. Simulation results on both ac to dc converters topologies with power factor correction as a function of output power and SE-LA line inductance impedance are presented and compared.

Nomenclature

V_{alt}	Alternator EMF voltage (V rms)
I_{alt}	Alternator current (A rms)
I_{alt}*	Alternator current command (A rms)
R_{alt}	Alternator winding resistance (Ω)
L_{alt}	Alternator winding inductance (Henries)
C_t	Tuning capacitance (mF)
C_{dc}	dc bus capacitance (mF)
R_{dc}	dc bus load resistance plus parasitic (Ω)
I_c	C_{dc} capacitance current (A rms)
I_{dc}	dc bus current (A rms)
V_t	Alternator terminal voltage (V)
V_{AB}	Rectifier voltage across nodes A and B (V)
XL_{alt}	Alternator inductive impedance (per unit)
XC_t	Tuning capacitor impedance (Ω)
$V_{ripple,p\text{-}p}$	dc bus peak-to-peak ripple (V peak-to-peak)
$V_{alt\text{–}peak}$	Time index during navigation
f	Alternator electrical frequency (Hz)
K	Current tolerance band scaling constant

I. Introduction

NASA Glenn Research Center (GRC) for years has been actively involved in the research and development of Stirling engines as an energy source for future NASA space exploration missions. These Stirling engine range in power levels from the 55 Watt Technology Demonstrator Converter (TDC) to the 12.5 kW Space Power Research Engine (SPRE). In more recent space mission studies, with power level requirement of approximately 100 kW, an array of high power Stirling Engines in the order of 70 kW each has also been considered.

Stirling engines typically possess two major moving parts, the displacer and the piston, both powered by thermal energy. To convert this thermal energy into electricity a linear alternator is attached to the piston to produce a single phase sinusoidal voltage waveform proportional to the piston amplitude (ref. 1) at a specific electric frequency.

Since all Stirling Engines-Linear Alternators perform at low electrical frequencies (less or equal to 100 Hz), exploration missions that can employ these engines as the energy source will likely use dc power management and distribution (PMAD) system instead of an ac PMAD system to save space and weight. If an ac PMAD were considered for a space mission, heavy transformers and filters will be necessary at each load to obtain dc power due to the low frequency electrical generation of the Stirling engine. These elements will make the ac PMAD system too big, heavy and impractical for any space mission. Therefore, an ac to dc converter is applied right at the output of the Stirling Engine-Linear Alternator to obtain a dc PMAD system. There are two types of ac to dc converters that can be employed, one converter is a passive full bridge diode rectifier as shown in figure 1, and the other converter is an active switching full bridge rectifier as shown in figure 2.

A SE-LA has an EMF voltage (V_{alt}) in series with the winding resistance (R_{alt}) and inductance (L_{alt}), (see figs. 1 and 2). The presence of the alternator winding inductance (L_{alt}) creates a phase lag of the current with respect to voltage at its output terminal (V_t), causing a reduction in power factor to values lower than one. In order to keep power factor close to unity, both ac to dc converters topologies implement power factor correction. In the case of the passive full bridge diode rectifier, a capacitor (C_t) connected in series, known as the tuning capacitor, will counteract the inductive reactance effect by putting an equal but opposite reactance at a specific electrical frequency resulting in an increase of the SE-LA power factor. For the active full bridge switching rectifier, power factor correction is achieved by controlling the switching of the MOSFETS.

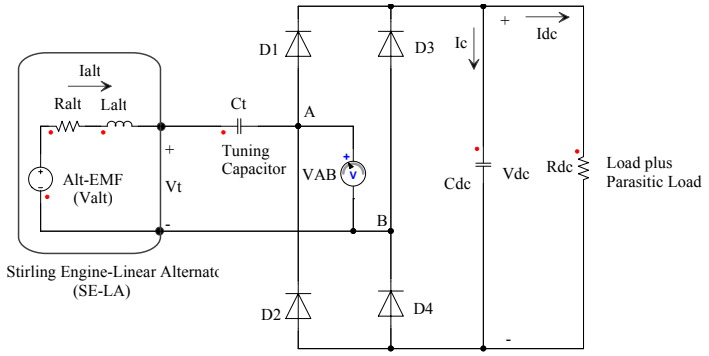

Figure 1.—Passive full bridge diode rectifier with tuning capacitors for power factor correction (PFC).

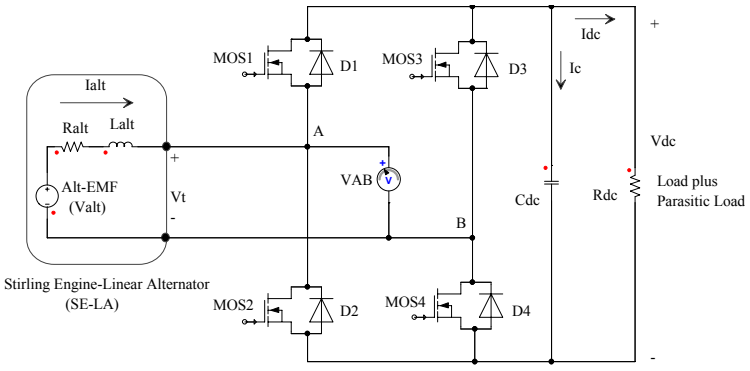

Figure 2.—Active full bridge switching rectifier.

Both topologies of ac to dc conversion plus Power Factor Correction (PFC) have their own advantages and disadvantages with respect to exploration missions. This paper discusses those advantages and disadvantages as well as their power factor correction methods and the topology impact on overall mass for exploration spacecraft. In addition, simulations results on both ac to dc converters topologies with PFC as a function of output power and SE-LA inductance (L_{alt}) impedance are presented and compared.

II. Passive Full Bridge Diode Rectifier with PFC

The passive full bridge diode rectifier with a tuning capacitor (C_t) for PFC has been the historical topology of choice for many Stirling engine research and development units, because they are simple to design, robust, efficient and easy to build. Essential to the Stirling Engine is the parasitic load control system which works together with the diode rectifier to regulate the dc voltage and control the Stirling piston stroke (X_p). During normal operation, the Stirling engine delivers constant power; therefore, the parasitic load controller will be used add or subtract parasitic loads depending upon the load demand.

To design a full bridge diode rectifier applied to a Stirling engine, three areas must be considered:

1) Diode voltage and current rating
2) dc capacitance (C_{dc}) voltage rating and value
3) Tuning capacitor (C_t) voltage rating and value

The diode voltage will be rated based on the regulated dc bus, typically $1.5\times V_{dc}$ or more, and its current rating is based on the rated power of the total dc load, usually $1.5\times I_{dc}$ or more. The C_{dc} voltage rating is also based on the

regulated dc bus (1.5×V_{dc} or more) and its value of C_{dc} depends on the amount of voltage ripple that the dc loads will accept. The larger the C_{dc} capacitance, the smaller the ripple at the dc bus. An approximate value of capacitance needed given the desired peak-to-peak voltage ripple ($V_{ripple,\,p-p}$) can be expressed as follows:

$$C_{dc} = \frac{I_{dc}}{4\pi * f * V_{ripple,p-p}} \tag{1}$$

where I_{dc} is the maximum dc load current and f is the electrical ac frequency of the SE-LA (ref. 2).

The tuning capacitor (C_t) rating will be based on the linear alternator terminal voltage (V_t) and the dc bus voltage (V_{dc}). The tuning capacitor voltage can be expressed as

$$V_{C_t} = V_t - V_{dc} \tag{2}$$

and when operating closed to unity power factor V_t can be expressed as

$$V_t = V_{alt} - V_{Lalt} \tag{3}$$

where V_{alt} is the alternator-EMF voltage, V_{Lalt} is the winding inductance voltage ($V_{Lalt} = \omega L_{alt} \times I_{alt}$) assuming that the alternator winding resistance (R_{alt}) is negligible. Therefore, the voltage rating for the tuning capacitor will be

$$V_{C_t} = V_t - V_{alt} - V_{dc} \tag{4}$$

The tuning capacitor value depends mainly on the linear alternator winding inductance value (L_{alt}) and the linear alternator electrical frequency (f). Therefore, the value of C_t can be obtained using:

$$C_t = \frac{1}{(2\pi * f)^2 L_{alt}} \tag{5}$$

By adding a properly sized tuning capacitor (C_t) in series with the alternator inductance (L_{alt}), the whole electrical system emulates a resistive load and the following benefits can be achieved:

1) Alternator current will be in phase with the alternator EMF voltage.
2) High current spikes at the rectification diodes are eliminated.
3) Peak current and hence EMI is reduced.
4) Current harmonics are reduced.
5) Significant reduction in reactive power resulting in better use of the Stirling Engine delivered power.
6) Power factor is close to unity.

Figure 3 shows the simulated results of a 70 kW/100 Hz/400 Vdc Stirling engine using a passive full bridge diode rectifier with a passive PFC topology. This shows that by adding a series capacitor, the current will closely follow the voltage resulting in a power factor close to unity. This is significantly better than if no tuning capacitor is used which can produce high current spikes (ref. 3). Note that the dc bus is being held at 400 Vdc with approximately 40 V peak-to-peak ripple (10% ripple).

By observing the alternator current waveform in figure 3 and its frequency spectrum in figure 4, it can be seen that the current in not purely sinusoidal even if a tuned capacitor is applied. A reason for this alternator current distortion or higher harmonics components can

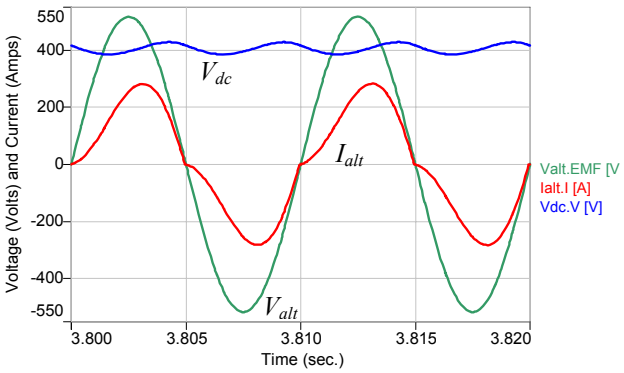

Figure 3.—Case no. 1: SE-LA output voltage (V_{alt}), current (I_{alt}) and dc voltage (V_{dc}), L_{alt} = 3.0 mH, XL_{alt} = 1 p.u.

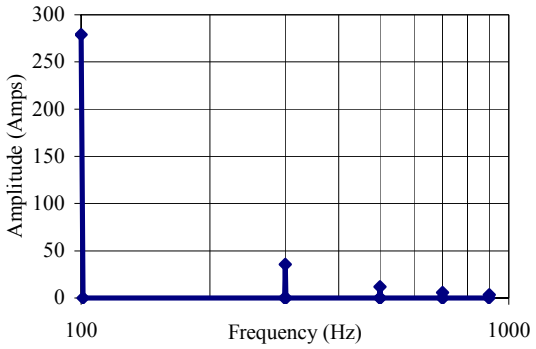

Figure 4.—Case no. 1: I_{alt} frequency spectrum for L_{alt} = 3.0 mH or XL_{alt} = 1 p.u.

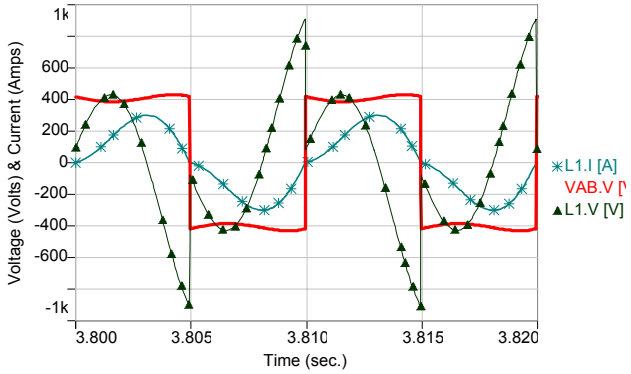

Figure 5.—Case no. 1: SE-LA inductance voltage (V_{Lalt} = L1.V) and current (I_{Lalt} = I_{alt} = L1.I).

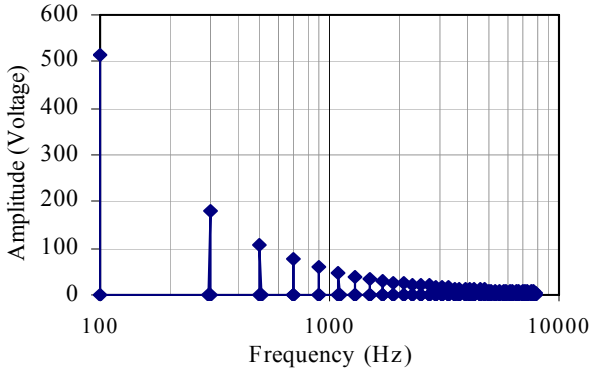

Figure 6.—V_{AB} frequency spectrum.

be attributed to the inductance value of the alternator windings (L_{alt}) and the bridge diode commutation action. Based on the full bridge diode rectifier shown on
figure 1, diodes D1 and D4 are conducting at the positive cycle of V_{alt} while D2 and D3 conduct during the negative cycle of V_{alt}. Every time a diode pair commutation occurs, voltage across V_{AB} abruptly changes from V_{dc} to $-V_{dc}$ and vice versa (fig. 5). This quick change of voltage, which can be approximated as a square voltage waveform, contains multiple voltage harmonic components derived from the 100 Hz fundamental frequency (fig. 6). These voltage harmonics can generate multiple alternator current harmonics, and the amount and magnitude of these current harmonics greatly depend on the impedance value of the alternator inductance. The impedance of the alternator inductance can be expressed as

$$XL_{alt} = j\omega L_{alt} \qquad (6)$$

where ω is equal to $2*\pi*f$.

The bigger the inductance value, the bigger the impedance, XL_{alt}. Subsequently, the I_{alt} current harmonics components will be greatly attenuated or blocked from circulation due to the high impedance path. This harmonic attenuation produces a more sinusoidal current wave shape thereby allowing the Stirling system power factor to be close to unity. For the tuning capacitor (C_t) impedance, its effect is totally opposite to SE-LA inductance impedance. The C_t instead creates a lower impedance path inversely proportional to the current harmonics frequencies ($XC_t = 1/(j\omega C_t)$). Therefore, no high frequency attenuation will be induced by the capacitor. The purpose of the tuning capacitor is to cancel the phase lag between the output current and voltage of the SE-LA at the fundamental alternator frequency.

A. Passive Full Bridge Rectifier with PFC Simulations Results

Table 1, in conjunction with figures 3, 4, 7, and 8, shows the simulations results of three different cases of alternator inductive impedance and its effects on the alternator current distortion, the current harmonics and the system power factor. For each of these cases the base power is 70 kW, the dc bus (V_{dc}) is 400 Vdc, and 100 Hz for the electrical frequency. For case no. 1 the alternator inductance impedances is 1per unit (XL_{alt} = 1 p.u.), for case no. 2, XL_{alt} is ten times the per unit value (10 p.u.), and case no. 3 is one tenth of the per unit value (0.1 p.u.). After the simulations and evaluations among all the three cases, the most favorable operating condition is case no. 2, when the SE-LA XL_{alt} is ten times the p.u. value or the inductance is approximately 30 mH (see fig. 7). This inductance value is high enough to create a high impedance path to suppress the current harmonics, a low THD and a power factor very close to one. For case no. 3 (see also fig. 8), when XL_{alt} equals one tenth the

p.u. value (0.1 p.u.) or its inductance is 0.3 mH, the impedance path is much lower allowing the presence of current harmonics in I_{alt}, causing a distorted current waveform (higher THD) and producing a lower power factor.

In summary, when employing a Stirling engine system that uses a passive full bridge diode rectifier with tuning capacitors for PFC, it is advantageous for the designer to maximize the inductance value on the alternator windings. A large inductance guarantees minimum alternator current distortion due to harmonics and a power factor close to one. Another benefit of large alternator inductance (L_{alt}) is that the capacitance value needed for the tuning capacitors to compensate for the inductance effect at the alternator fundamental frequency is much less than the cases of low L_{alt}, see equation (5) and table 1. Low values of C_t result in lower mass penalties for any exploration mission.

TABLE 1.—COMPARATIVE CASES OF THE SE-LA WINDING INDUCTANCE (L_{alt}) WHEN USING PASSIVE RECTIFICATION

	Case no. 1	Case no.2	Case no. 3
XL_{alt} (p.u.)	1	10	0.1
Alternator inductance (mH)	3.029	30	0.3
Tuning capacitor (C_t) (mF)	0.836	0.08	8.0
Power factor	0.97	0.995	0.81
Ialt THD	10.3	5.20	61.64
S-base (kW)	70	70	70
V-base (V)	365	365	365
Vdc (V)	400	400	400
Fundamental frequency(Hz)	100	100	100

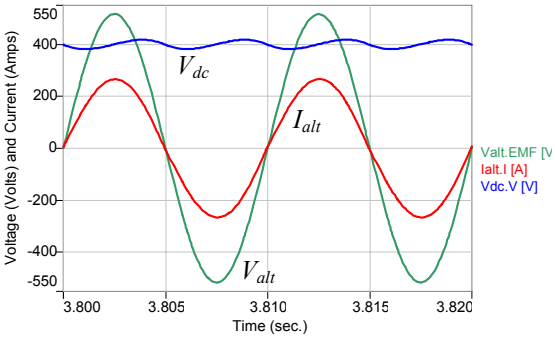

Figure 7.—SE-LA output voltage (V_{alt}), current (I_{alt}) and dc voltage (V_{dc}), L_{alt} = 30.0 mH, XL_{alt} = 10 p.u.

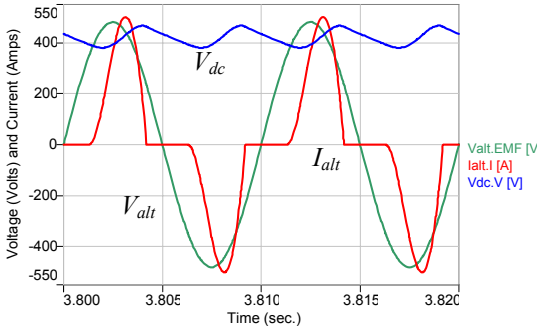

Figure 8.—SE-LA output voltage (V_{alt}), current (I_{alt}) and dc voltage (V_{dc}), L_{alt} = 0.30 mH, X_{Lalt} = 0.1 p.u.

III. Active Full Bridge Rectifier (AFBR) with Active Power Factor Correction (APFC)

With the technological advancement in electronics over the last couple of decades and new developments in controls, the use of MOSFETs as a high power, fast switching device has revolutionized the power electronics arena. These new advancements have introduced an alternative method that can be applied to the SE-LA ac to dc rectification and PFC efforts. Figure 2 shows this new method which is called as Active Full Bridge Rectifier (AFBR) with APFC. A major advantage of this topology is that the tuning capacitor (C_t) for power factor correction is no longer needed. Power factor correction is performed by switching MOSFET 1 through 4 in a combinative sequence such that the alternator current (I_{alt}) falls in phase with the alternator EMF voltage (V_{alt}).

Table 2 shows a list of electrical parameters that describes the AFBR with APFC topology. Here, the alternator EMF voltage peak (V_{alt}-peak), the alternator inductance (L_{alt}), and the alternator impeadance (X_{alt}) are limited to a certain range of values to assure the proper performance of the AFBR topology. For this case, the alternator EMF voltage peak is kept below the dc bus voltage, because the AFBR topology works better in voltage boost mode than in voltage buck mode. Since the alternator EMF peak voltage is being kept below 400 Vdc (V_{alt} < 283 V), the alternator current has to be high enough to supply the required 70 kW. This imposes a limitation to the SE-LA inductance value and the inductive impedance (XL_{alt}) for the AFBR to work. Both of this need to be kept low, otherwise the alternator current will be to slow to react to the MOSFETs rapid switching and the PF will be less than one.

The active power factor correction main control scheme that synchronizes the activation of the AFBR MOSFETs and makes the alternator current follow the alternator EMF voltage is called *tolerance band control* (ref. 2). This type of control uses a reference current signal (I_{alt}*), where the actual current (I_{alt}) is compared with the tolerance band around the reference current (see fig. 9(a)). If the actual current tries to go beyond the upper tolerance, the control algorithm of the AFBR dictates the next appropriate switching command state to reduce the I_{alt} current. The opposite switching occurs if the actual current needs to be increased or tries to go below the lower tolerance band.

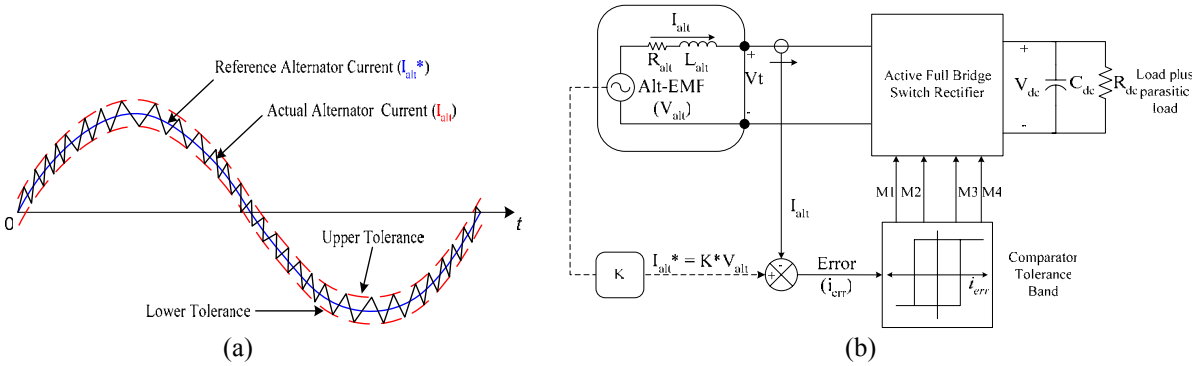

Figure 9.—Tolerance band control for APFC.

To acquire the reference current signal (I_{alt}*) in a simulation environment, V_{alt} can be used and scaled by a constant K to the amount of current needed for the Stirling engine to supply the demanded power (fig. 9(b)). In reality, the internal EMF voltage (V_{alt}) is not available on most Stirling engine designs; however, it can be derived from the Stirling piston position signal (ref. 4). The switching frequency of the AFBR MOSFETs depends on how fast the current changes from the upper limit to the lower limit and vice versa, which, in turn depends on the L_{alt} inductance value. Moreover, the switching frequency does not remain constant, but varies along the current waveform.

TABLE 2.—ELECTRICAL DESIGN PARAMETER FOR A DEEP SPACE EXPLORATION MISSION

Fixed design parameter		Dependent or variable parameters	
Parameter	Value	Parameter	Value
Power output (P_{out})	70 kW	$V_{alt\text{-}peak}$	< V_{dc}
dc bus (V_{dc})	400 Vdc	I_{alt}	P_{out}/V_{alt}
Alternator frequency	100 Hz	L_{alt}	Low
		XL_{alt}	< 1 p.u.

There are many switching combinations that have been described in previous papers (refs. 4, 5, and 6). To keep AFBR simple in a high power Stirling system for exploration missions, only two switching sequences were simulated, studied and compared. One switching scheme turns on two MOSFETs at the same time and the second switching scheme turns on only one MOSFET. The two MOSFET switching scheme can have a better performance than the one MOSFET scheme in terms of counteracting the effect of the alternator inductance when XL_{alt} is closed to 1 p.u. When XL_{alt} is close to 1 p.u., the alternator inductance is large enough to slow down the flow of alternator current, especially when the current needs to be increased, thereby affecting the power factor correction effort. To have a quick and almost linear change in alternator current a large voltage across the alternator inductance must be applied. To achieve this, the two MOSFET scheme turns on the switches that can use the dc voltage bus (V_{dc}) in series and at the same polarity orientation with the alternator EMF voltage (V_{alt}) so that I_{alt} can linearly rise without the slowdown effect of the alternator inductance, see figure 9(a).

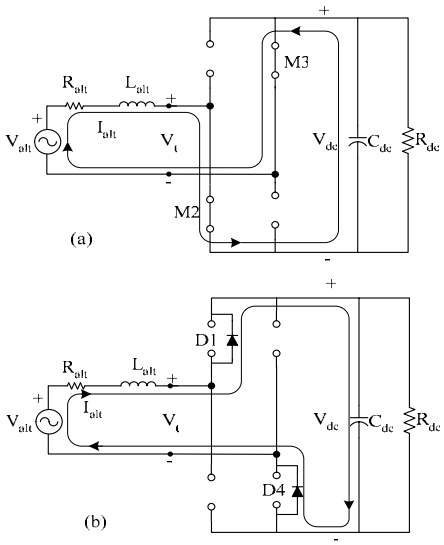

Figure 10.—Two MOSFETs switching scheme when V_{alt} polarity is positive.

In the case when XL_{alt} is well below 1 p.u., the alternator inductance is low enough to use the one MOSFET switching scheme. With very low alternator inductance, a quick and linear increase in the alternator current can be made by simply turning on only one MOSFET making the voltage across the inductor equal to the alternator EMF voltage. Even though the two MOSFETs switching scheme can be applied at low alternator inductance it is more efficient and reliable, for space missions, to use the one MOSFET scheme. One MOSFET scheme cuts switching and conduction losses in half when used in conjunction with diodes with small forward voltage drop.

As mentioned before, the AFBR topology with APFC will primarily use the two switching schemes in order to follow the reference current (I_{alt}*) signal by increasing and reducing the actual alternator current. Table 3 depicts the switching states for both switching scheme methods as a function of the alternator EMF voltage (V_{alt}) polarity and the effect on the terminal voltage (V_t) and the alternator current (I_{alt}). For the two MOSFET switching scheme, figure 10 and table 3 show how the alternator current rises and falls while the alternator EMF voltage is in the

positive half cycle. When MOSFETs M2 and M3 are turned on, V_t is equal to $-V_{dc}$ (fig. 10(a)), thus the voltage across the alternator inductor will be the sum of the alternator EMF voltage (V_{alt}) plus the dc bus voltage (V_{dc}). This will be enough voltage potential to counteract the large alternator inductance value and create an increase in the alternator current up to the upper tolerance current of the tolerance band control system (fig. 9). When the upper tolerance has been reached, the alternator current is reduced by turning off M2 and M3 and letting the current flow though diodes D1 and D4 charging the dc bus capacitor (C_{dc}), see figure 10(b). When the alternator current reaches the lower tolerance band, MOSFETs M2 and M3 will turn on to start the cycle again. The same thing happens when the alternator EMF voltage is in the negative half cycle, but in this case MOSFETS M1 and M4 will be turned on to increase the alternator current and diodes D3 and D2 will be used to reduce the current.

TABLE 3.—SWITCHING SEQUENCE STATES FOR ACTIVE FULL BRIDGE RECTIFIER WITH PFC

	Switching scheme no. 1: Two MOSFET switching				Switching scheme no. 2: One MOSFET switching			
V_{alt} polarity	MOSFET or diode on	V_t (V_{AB})	I_{alt} effect	State no.	MOSFET or diode on	V_t (V_{AB})	I_{alt} effect	State no.
+	M2, M3	$-V_{dc}$	Increase	1	M2, D4	0	Increase	A
+	D1, D4	V_{dc}	Decrease	2	D1, D4	V_{dc}	Decrease	B
+	N/A	N/A	N/A	N/A	M3, D1	0	Increase	C
–	M1, M4	V_{dc}	Increase	3	M1, D3	0	Increase	D
–	D2, D3	$-V_{dc}$	Decrease	4	D2, D3	$-V_{dc}$	Decrease	E
–	N/A	N/A	N/A	N/A	M4, D2	0	Increase	F

Figure 11 and table 3 show how the current rises and falls on the alternator while the alternator EMF voltage is in the positive half cycle for the one MOSFET switching scheme. When MOSFET M2 is turned on, V_t is zero volts (fig. 11(a)). Therefore, the voltage across the alternator inductor will be only the alternator EMF voltage (V_{alt}). This creates enough voltage potential to counteract the small alternator inductance value causing an increase in the alternator current up to the upper tolerance current of the tolerance band control system (fig. 9). When the upper tolerance has been reached the alternator current is reduced by turning off M2 and letting the current flow though diodes D1 and D4 charging the dc bus capacitor (C_{dc}) (fig. 11(b)). To alternate between MOSFETs while the alternator EMF is positive, M3 can be turned on instead of M2 to increase the alternator current. Turning on M3 will have the same effect on the alternator current, and when the current reaches the upper tolerance current of the tolerance band control system, M3 will be turned off and the current will flow through diodes D1 and D4 and fall. Once the alternator current reaches the lower tolerance band, either M2 or M3 will turn on to start the cycle again. The same thing happens when the alternator EMF voltage is in the negative half cycle but in this case MOSFETS M1 and M4 will be alternated on to increase the alternator current, and diodes D2 and D3 will be used to reduce the current.

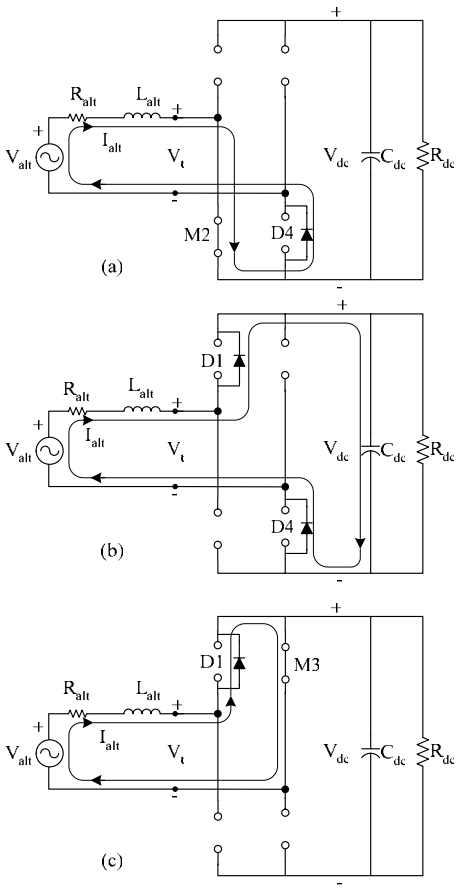

Figure 11.—One MOSFET switching scheme when V_{alt} polarity is positive.

A. Active Full Bridge Rectifier (AFBR) with APFC Simulation Results at Two L_{alt} Cases

To demonstrate the effect of the alternator inductance on both switching schemes of the AFBR topology, two cases of alternator impedance were simulated and evaluated. The first set of simulations XL_{alt} is set to be 1 per unit and the second set of simulations is when X_{Lalt} equals to one tenth of the per unit impedance (0.1 p.u.). The impedance condition of ten times the

per unit value (10 p.u.) was not simulated due to the fact that the alternator inductance will be too large and the alternator current response will be too slow to adjust when using the AFBR with APFC topology. Table 4 in conjunction with figures 12 to 21 shows the influence the SE-LA inductance has over the power factor correction and the alternator current waveform distortion at the two different switching cases. Again, each of these switching schemes use the requirements stipulated in table 2.

The simulation results of the two MOSFET switching scheme when the alternator inductive impedance is set at 1 per unit (L_{alt} = 1.75 mH) are shown on table 4 and figures 12 to 14. Here the dc bus voltage is maintained at 400 V and the alternator current waveform follows the EMF voltage with some distortion in its wave shape thus producing a system a power factor of 0.97 (fig. 12). With XL_{alt} at 1 p.u., the active power factor correction seems to work properly, but not well enough to produce a distortion free alternator current waveform. This is due to the alternator inductive impedance slowing the alternator current response and hindering the proper performance of the current *tolerance band control* algorithm (fig. 9). This current slow down can also be seen in figure 13, in which V_{AB} (same as the alternator output terminal voltage, V_t) exhibits discontinued switching of the two MOSFETs. V_{AB} is used to vary the alternator current for PFC, and its value is set by the switching states of table 3 to provide the current *tolerance band control*. The V_{AB} discontinued switching is caused when the alternator current falls within the tolerance band of the control system for a long time without reaching either tolerance limits (fig. 9(a)) which causes an extended switching state because the current is not changing rapidly. Finally, the non sinusoidal shape of the alternator current leads to harmonics components and is shown in figure 14(a) with a total harmonic distortion of 9.8 percent.

TABLE 4.—SIMULATION RESULTS FOR BOTH AFBR SWITCHING SCHEMES

Parameter	Two MOSFET switching scheme		One MOSFET switching scheme	
XL_{alt}	1 p.u.	0.1 p.u.	1 p.u.	0.1 p.u.
L_{alt} (mH)	1.75	0.175	1.75	0.175
I_{alt} THD (%)	9.80	2.94	12.63	3.07
Power Factor	0.97	0.999	0.90	0.999
S base (kW)	70	70	70	70
V_{alt} base (V)	279	279	279	279
V_{dc} (V)	400	400	400	400
Frequency (Hz)	100	100	100	100

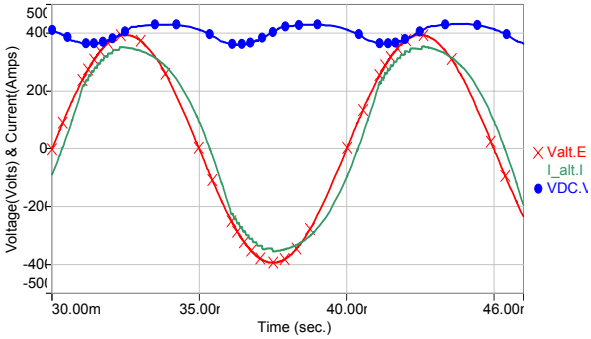

Figure 12.—V_{alt}, I_{alt} and V_{dc} waveforms for two MOSFETs switching scheme with XL_{alt} = 1 p.u.

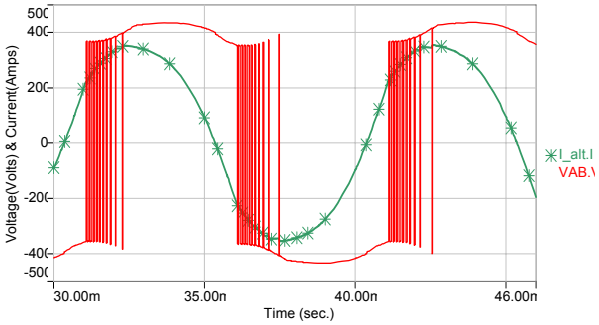

Figure 13.—I_{alt} and V_{AB} waveforms for two MOSFETs switching scheme with XL_{alt} = 1 p.u.

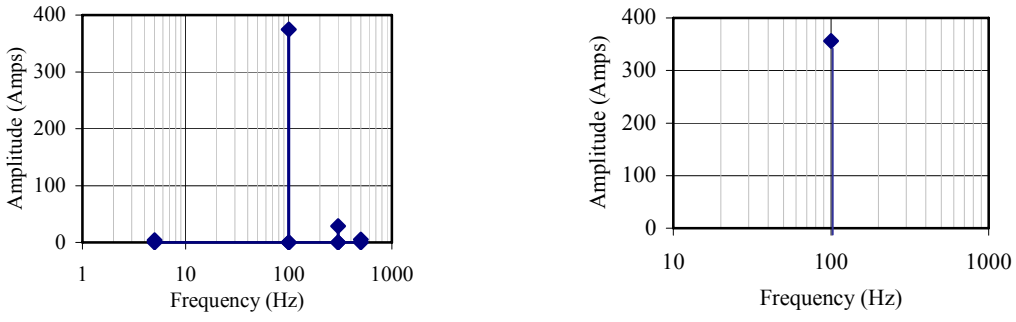

Figure 14.—I_{alt} frequency spectrum for two MOSFETs switching scheme (a) with X_{Lalt} = 1 p.u. and (b) XL_{alt} = 0.1 p.u.

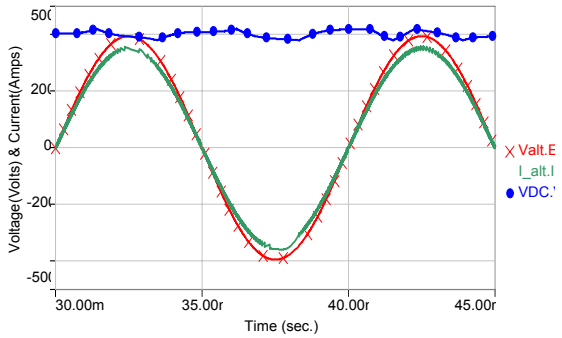

Figure 15.—V_{alt}, I_{alt}, and V_{dc} waveforms for two MOSFETs switching scheme with XL_{alt} = 0.1 p.u.

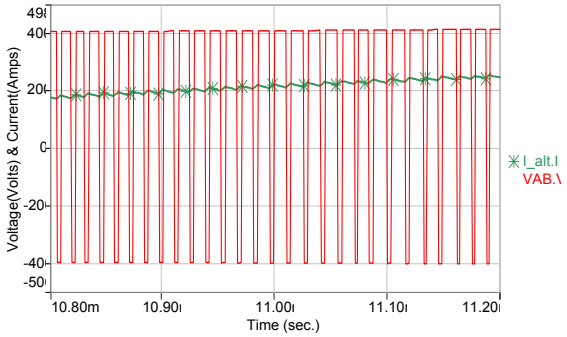

Figure 16.—I_{alt} and V_{AB} waveforms for Two MOSFETs switching scheme with XL_{alt} = 0.1 p.u.

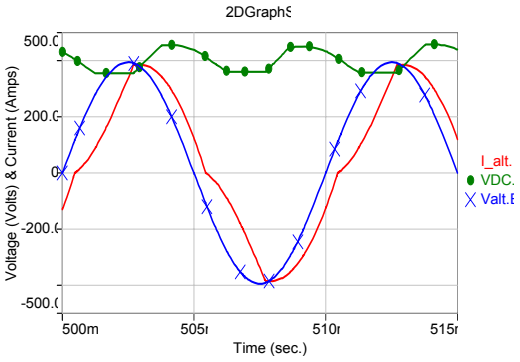

Figure 17.—V_{alt}, I_{alt}, and V_{dc} waveforms for one MOSFETs switching scheme with XL_{alt} = 1 p.u.

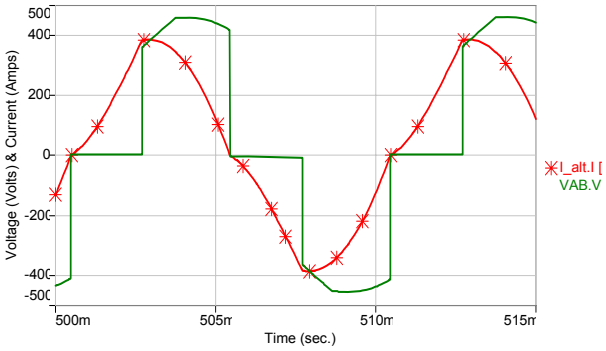

Figure 18.—I_{alt} and V_{AB} waveforms for two MOSFETs switching scheme with XL_{alt} = 1 p.u.

Figures 15, 16, and 14(a) shows the same 2 MOSFET switching scheme with the alternator inductive impedance at one tenth the per unit value or the inductance is 0.175 mH. Compared to the previous case, can be seen the major influence the alternator impedance has over the alternator current waveform. In this case, the alternator current precisely follows the EMF voltage with no current waveform distortion, increasing the power factor to 0.999 with a THD of 2.94 percent, while maintaining 400 V at the dc bus. Also, the current tolerance band control algorithm works during the entire current cycle as is shown in figure 15. Figure 16 also shows that the low alternator inductive impedance allows fast change in alternator current, proper operation of the current band control, and continuous switching of V_{AB} (or V_t) along the cycle. Finally, figure 14(b) shows only a single current component at 100 Hz, at the alternator electrical frequency.

Modeling results for the one MOSFET switching scheme with XL_{alt} = 1 p.u. can be seen in figures 17, 18, 19(a), and table 4. These figures depict the same behavior as the case of two MOSFETs switching scheme. The inductive impedance of one per unit produces an inductance large enough to slow down the alternator current and affect the current band control algorithm, reducing the power factor (0.9) and increasing the THD (12.63%). In comparison with the two MOSFET switching scheme with XL_{alt} = 1 p.u. (table 4), power factor and THD are higher due to the fact that only one MOSFET is switching and insufficient voltage across the alternator inductor results in a slow increase in the alternator current.

Results for the one MOSFET switching scheme with XL_{alt} = 0.1 p.u. are shown in figures 20, 21 and 19(b). Compared to the preceding case (one MOSFET and 1 p.u. impedance), one can see the major influence the alternator impedance has on the alternator current waveform. Here, the alternator current precisely follows the EMF voltage with no current waveform distortion making the power factor 0.999 with THD of 3.07 percent, while maintaining 400 V at the dc bus. Here the current tolerance band control algorithm works during the entire current cycle as is shown in figure 20. Figure 21 also shows that low alternator inductive impedance allows fast change in alternator current, proper operation of the current band control and continuous switching of V_{AB} (or V_t) along the cycle. Figure 19(b) shows a single current component at 100 Hz which is the same as the alternator electrical frequency.

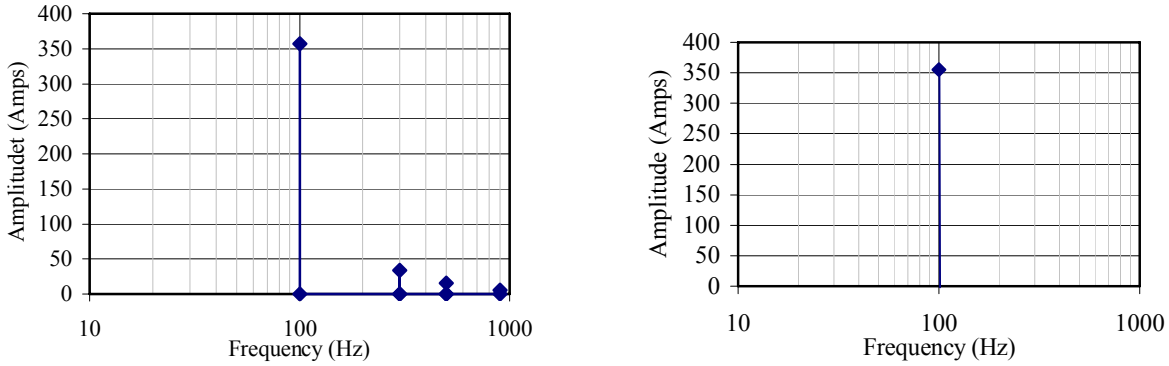

(a) (b)

Figure 19.—I_{alt} frequency spectrum for one MOSFETs switching scheme.

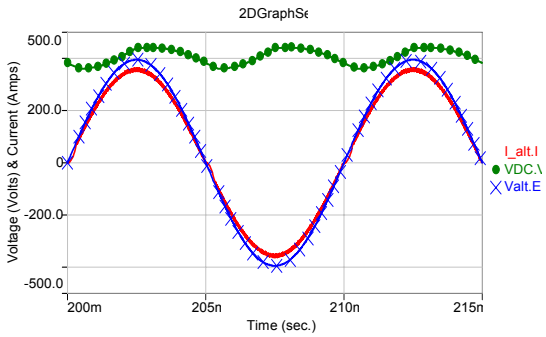

Figure 20.—V_{alt}, I_{alt}, and V_{dc} waveforms for one MOSFETs switching scheme with X_{Lalt} = 0.1 p.u.

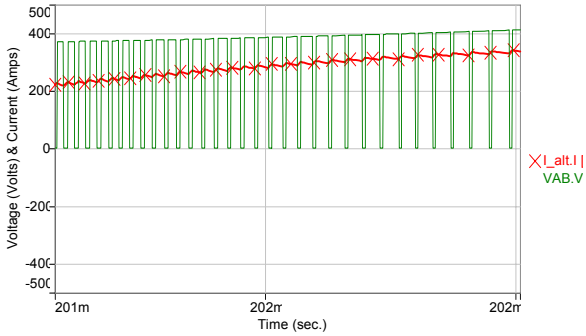

Figure 21.—I_{alt} and V_{AB} waveforms for two MOSFETs switching scheme with X_{Lalt} = 0.1 p.u.

As seen on table 4, when the alternator impedance is equal to 0.1XL_{alt}, both MOSFET switching schemes result in similar power factors and alternator current THD. Both schemes work very well, but the one MOSFET switching scheme has an advantage over the two MOSFET case; by only switching one MOSFET the AFBR with APFC topology becomes more efficient and reliable. One MOSFET switching cuts switching and conduction losses by half and the power diodes with low forward voltage drop are used for a greater length of time.

IV. Comparison Between Passive and Active Rectification with APFC for High Power Stirling

For a high power space exploration mission that uses a Stirling engine, careful consideration should be given to the type of ac to dc rectification topology to be applied. Both passive and active rectification with power factor correction has advantages and disadvantages, depending on the SE-LA winding inductance design. In addition, the simplicity of the design, robustness, reliability, efficiency, and mass will play an important role for the final design approach. In this section, advantages and disadvantages for passive and active rectification are described in terms of their performance and their design parameters.

A. Passive Rectification with Power Factor Correction

Passive rectification using full bridge diode rectifier is very simple. High voltage and high current diodes that are made for the severe environmental conditions of deep space have a low forward voltage (between 1 and 2 V) drop. This results in an efficiency reduction of about 3 percent.

The major disadvantage of the passive rectification approach is that it needs capacitors for power factor correction. Capacitors are very big, bulky and heavy. The level of capacitance needed for a high power Stirling is in the order of millifarads resulting in weight and volume impacts.

If a passive rectification design is finally considered as the topology of choice for any deep space mission, the best design will be influenced by the linear alternator design. Based on the simulations it can be concluded that a

SE-LA design that possess the largest possible winding inductance value (L_{alt}) will perform best when the diode bridge is applied. The benefits are:

1) Power factor close to one (see table 1 when L_{alt} = 30 mH)
2) Low current harmonics with minimum distortion (see table 1 when XL_{alt} = 10 p.u.)
3) High terminal voltage (V_t) due to large inductance.
4) Minimum capacitance weight.

B. Active Rectification with Active Power Factor Correction

The attractive feature that the active rectification topology brings is the total elimination of the tuning capacitor (C_t). By eliminating the tuning capacitors volume and mass are saved. Also, active rectification implies active closed loop control, allowing more accurate rectification and power factor correction can be achieved. However, some side effects results on the performance, reliability, robustness and simplicity of the active rectification design.

The efficiency of the active rectification topology is lower than the passive rectifier topology. To increase its efficiency, the number of parallel MOSFETs per switch will need to increase, resulting in an increase of the topology complexity, a reduction in reliability, and an increase of the controls and drive circuits needed for the MOSFETs.

If an active rectification design is finally considered as the topology of choice for any deep space mission, the best design will be influenced by the linear alternator design. Based on the on the simulations described in the previous sections, it can be concluded that a SE-LA that posses the lowest possible winding inductance value (L_{alt}) will perform best when the AFBR with APFC is applied. The benefits for this are:

1) Power factor close to one (see table 4 when L_{alt} = 0.175 mH)
2) Low current harmonics with minimum distortion (see table 4 when XL_{alt} = 0.1 p.u.)
3) No tuning capacitors (C_t)
4) No mass penalty due to the tuning capacitance

Table 5 shows the features of each rectifier topology and summarizes their respective strengths and weaknesses.

TABLE 5.—PARAMETRIC COMPARISON BETWEEN PASSIVE AND ACTIVE RECTIFICATION

Parameter	Passive rectification	Active rectification
Design	Simple	Complex
Reliability	High	Moderate
Controls	No	Yes
Weight due to tuning capacitor (C_t)	High	Zero
Tuning capacitor (C_t)	Yes	No
Terminal voltage (V_t)	High	Below V_{dc}
Power factor	0.999 for large L_{alt}	0.999 for low L_{alt}
Efficiency	~97%	~92%
L_{alt}	Large	Small

V. Conclusion

Stirling engines have been considered as a main power source for high power space exploration missions. The key factors, for its success is the efficient and reliable energy transfer, as well as a simple design configuration with minimum weight. The ac to dc rectifier with power factor correction is one of the subsystems that can impact the entire Stirling system.

Two types of ac to dc rectifiers have been simulated and compared as a preliminary step in evaluating the design of a mission PMAD system. When applying either passive or active rectification in a Stirling system, the SE-LA winding inductance (L_{alt}) plays a key role in the level of performance of each rectification topology. It was demonstrated that a SE-LA with a large winding inductance (at the level of 10 times the per unit inductive impedance value), a passive ac to dc diode rectifier will provide a simple, reliable and efficient design solution. Simulations show that its power factor is very close to one with almost no distortion in the alternator current. Since

the tuning capacitor (C_t) can create a big penalty in terms of weight and space, this must be kept to a minimum by designing the SE-LA with the largest alternator inductance possible. Passive rectification applied to a SE-LA with low winding inductance will have lower power factor with distortion in the alternator current and the tuning capacitor will be large in value and size.

Active rectification eliminates the PFC tuning capacitors; however, this topology requires the SE-LA to be designed with very low inductance, so that active rectification can work properly. In an active high power rectifier design, each switch should consist of an array of MOSFETs which can increase the complexity as well as reduce the converter reliability. Simulations have demonstrated that the best design for an active rectification topology is one that uses the one MOSFET switching scheme (instead of two) where the efficiency is maximized. Clearly, this one switching scheme for rectification and PFC can only be applied if and only if the SE-LA winding inductance is kept to a minimum or at approximately one tenth of the SE-LA inductive impedance.

References

1. Reagan, T.F., Gerber, S.S., Roth, M.E., "Development of a Dynamic, End-to-End Free Piston Stirling Convertor Model," NASA/TM—2004-21941.
2. Mohan, N., Undeland, T.M., Robbins, W.P., Power Electronics: Converters, Applications and Design, 1st ed., Wiley, New York, 1989, chap. 6, 17.
3. Millman, J., Micro-electronics: Digital and Analog Circuits and Systems, 1st ed., McGraw-Hill, New York, 1979, Chap. 10.
4. Gerber, S.S., Jamison, M., Regan, T.M., Roth, M.E. "Advanced Controller for the Free-Piston Stirling Convertor," AIAA–2004–5519.
5. Salmon, J.C., "Techniques for Minimizing the Input Current Distortion of Current-Controlled Single-Phase Boost Rectifiers," *IEEE Transactions On Power Electronics,* vol. 8, no. 4, pp. 509–520, October 1993.
6. Enjeti, P.N., Martinez, R., "A High performance Single Phase AC to DC Rectifier with Input Power Factor Correction," IEEE 0–7803–0982-0/93, pp. 190–195.

REPORT DOCUMENTATION PAGE

Form Approved
OMB No. 0704-0188

1. AGENCY USE ONLY (*Leave blank*)	2. REPORT DATE	3. REPORT TYPE AND DATES COVERED
	March 2006	Technical Memorandum

4. TITLE AND SUBTITLE

Single Phase Passive Rectification Versus Active Rectification Applied to High Power Stirling Engines

5. FUNDING NUMBERS

WBS–22–319–20–M1

6. AUTHOR(S)

Walter Santiago and Arthur G. Birchenough

7. PERFORMING ORGANIZATION NAME(S) AND ADDRESS(ES)

National Aeronautics and Space Administration
John H. Glenn Research Center at Lewis Field
Cleveland, Ohio 44135–3191

8. PERFORMING ORGANIZATION REPORT NUMBER

E–15402

9. SPONSORING/MONITORING AGENCY NAME(S) AND ADDRESS(ES)

National Aeronautics and Space Administration
Washington, DC 20546–0001

10. SPONSORING/MONITORING AGENCY REPORT NUMBER

NASA TM—2006-214045
AIAA–2005–5687

11. SUPPLEMENTARY NOTES

Prepared for the Third International Energy Conversion Engineering Conference sponsored by the American Institute of Aeronautics and Astronautics, San Francisco, California, August 15–18, 2005. Responsible person, Walter Santiago, organization code RPE, 216–433–8486.

12a. DISTRIBUTION/AVAILABILITY STATEMENT

Unclassified - Unlimited
Subject Category: 20

Available electronically at http://gltrs.grc.nasa.gov

This publication is available from the NASA Center for AeroSpace Information, 301–621–0390.

12b. DISTRIBUTION CODE

13. ABSTRACT ***(Maximum 200 words)***

Stirling engine converters are being considered as potential candidates for high power energy conversion systems required by future NASA explorations missions. These types of engines typically contain two major moving parts, the displacer and the piston, in which a linear alternator is attached to the piston to produce a single phase sinusoidal wave-form at a specific electric frequency. Since all Stirling engines perform at low electrical frequencies (less or equal to 100 Hz), space explorations missions that will employ these engines will be required to use DC power management and distribution (PMAD) system instead of an AC PMAD system to save on space and weight. Therefore, to supply such DC power an AC to DC converter is connected to the Stirling engine. There are two types of AC to DC converters that can be employed, a passive full bridge diode rectifier and an active switching full bridge rectifier. Due to the inherent line inductance of the Stirling Engine-Linear Alternator (SE-LA), their sinusoidal voltage and current will be phase shifted producing a power factor below 1. In order to keep power the factor close to unity, both AC to DC converters topologies will implement power factor correction. This paper discusses these power factor correction methods as well as their impact on overall mass for exploration applications. Simulation results on both AC to DC converters topologies with power factor correction as a function of output power and SE-LA line inductance impedance are presented and compared.

14. SUBJECT TERMS

Stirling engines; AC to DC rectifier; Power factor; Generator

15. NUMBER OF PAGES

18

16. PRICE CODE

17. SECURITY CLASSIFICATION OF REPORT	18. SECURITY CLASSIFICATION OF THIS PAGE	19. SECURITY CLASSIFICATION OF ABSTRACT	20. LIMITATION OF ABSTRACT
Unclassified	Unclassified	Unclassified	